

# Design of a thin disk amplifier with extraction during pumping for high peak and average power Ti:Sa systems (EDP-TD)

Vladimir Chvykov,<sup>1,\*</sup> Roland S. Nagymihaly,<sup>1</sup> Huabao Cao,<sup>1</sup> Mikhail Kalashnikov,<sup>1,2</sup>  
and Karoly Osvay<sup>1</sup>

<sup>1</sup>ELI-Hu Nkft., Dugonics ter 13, H-6720 Szeged, Hungary

<sup>2</sup>Max-Born-Institut für Nonlinear Optics and Short Pulse Spectroscopy, Max-Born-Strasse 2a, 12489 Berlin, Germany

\*Vladimir.chvykov@eli-alps.hu

**Abstract:** Combination of the scheme of extraction during pumping (EDP) and the Thin Disk (TD) technology is presented to overcome the limitations associated with thermal cooling of crystal and transverse amplified spontaneous emission in high average power laser systems based on Ti:Sa amplifiers. The optimized design of high repetition rate 1-10 PW Ti:Sapphire EDP-TD power amplifiers are discussed, including their thermal dynamic behavior.

©2016 Optical Society of America

**OCIS codes:** (140.3280) Laser amplifiers; (140.7090) Ultrafast lasers; (140.3590) Lasers, titanium.

---

## References and links

1. Y. Chu, Z. Gan, X. Liang, L. Yu, X. Lu, C. Wang, X. Wang, L. Xu, H. Lu, D. Yin, Y. Leng, R. Li, and Z. Xu, "High-energy large-aperture Ti:sapphire amplifier for 5 PW laser pulses," *Opt. Lett.* **40**(21), 5011–5014 (2015).
2. G. A. Mourou, N. J. Fisch, V. M. Malkin, Z. Toroker, E. A. Khazanov, A. M. Sergeev, T. Tajima, and B. Le Garrec, "Exawatt-Zettawatt pulse generation and applications," *Opt. Commun.* **285**(5), 720–724 (2012).
3. G. Mourou, T. Tajima, and S. Bulanov, "Optics in the relativistic regime," *Rev. Mod. Phys.* **78**(2), 309–371 (2006).
4. W. P. Latham, A. Lobad, T. C. Newell, D. Stalnaker, and C. Phipps, "6.5 kW, Yb:YAG Ceramic Thin Disk Laser," *AIP Conf. Proc.* **1278**, 758–764 (2010).
5. J. Tümmler, R. Jung, H. Stiel, P. V. Nickles, and W. Sandner, "High-repetition-rate chirped-pulse-amplification thin-disk laser system with joule-level pulse energy," *Opt. Lett.* **34**(9), 1378–1380 (2009).
6. C. J. Saraceno, F. Emaury, O. H. Heckl, C. R. E. Baer, M. Hoffmann, C. Schriber, M. Golling, T. Südmeyer, and U. Keller, "275 W average output power from a femtosecond thin disk oscillator operated in a vacuum environment," *Opt. Express* **20**(21), 23535–23541 (2012).
7. C. J. Saraceno, F. Emaury, C. Schriber, M. Hoffmann, M. Golling, T. Südmeyer, and U. Keller, "Ultrafast thin-disk laser with 80  $\mu$ J pulse energy and 242 W of average power," *Opt. Lett.* **39**(1), 9–12 (2014).
8. C. Teisset, M. Schultze, R. Bessing, M. Haefner, S. Prinz, D. Sutter, and T. Metzger, "300 W Picosecond Thin-Disk Regenerative Amplifier at 10 kHz Repetition Rate," in *Advanced Solid-State Lasers Congress Postdeadline*, G. Huber and P. Moulton, eds., OSA Postdeadline Paper Digest (online) (Optical Society of America, 2013), paper JTh5A.1.
9. J.-P. Negel, A. Voss, M. A. Ahmed, D. Bauer, D. Sutter, A. Killi, and T. Graf, "1.1 kW average output power from a thin-disk multipass amplifier for ultrashort laser pulses," *Opt. Lett.* **38**(24), 5442–5445 (2013).
10. J. Speiser, "Scaling of thin-disk lasers-influence of amplified spontaneous emission," *J. Opt. Soc. Am. B* **26**(1), 26 (2009).
11. V. Chvykov, J. Nees, and K. Krushelnick, "Transverse amplified spontaneous emission: The limiting factor for output energy of ultra-high power lasers," *Opt. Commun.* **312**, 216–221 (2014).
12. M. P. Kalachnikov, V. Karpov, H. Schönngel, and W. Sandner, "100 – terawatt titanium-sapphire laser system," *Laser Phys.* **12**(2), 368–374 (2002).
13. H. Qiu, P. Yang, J. Dong, P. Deng, J. Xu, and W. Chen, "The influence of Yb concentration on laser crystal Yb:YAG," *Mater. Lett.* **55**, 1–7 (2002). A. Peter, "Schulz, Scott R. Henion, "Liquid-Nitrogen-Cooled Ti: A12 O3 Laser," *IEEE J. Quantum Electron.* **27**(4), 1039–1047 (1991).
14. [http://inventions.umich.edu/technologies/6154\\_thin-disk-extraction-during-pumping-laser-amplifier](http://inventions.umich.edu/technologies/6154_thin-disk-extraction-during-pumping-laser-amplifier)

15. V. Chvykov, V. Yanovsky, S.-W. Bahk, G. Kalintchenko, and G. Mourou, "Suppression of parasitic lasing in multi-pass Ti:sapphire amplifiers," in Proceedings of the OSA Technical Digest, CLEO 2003, paper CWA34 (2003).
16. V. Chvykov and K. Krushelnick, "Large aperture multi-pass amplifiers for high peak power lasers," *Opt. Commun.* **285**(8), 2134–2136 (2012).
17. V. Chvykov, M. Kalashnikov, and K. Osvay, "Final EDP Ti:Sapphire Amplifiers for ELI Project," SPIE Proceeding, LOO 9515–18 (2015).
18. F. Plé, M. Pittman, G. Jamelot, and J. P. Chambaret, "Design and demonstration of a high-energy booster amplifier for a high-repetition rate petawatt class laser system," *Opt. Lett.* **32**(3), 238–240 (2007).
19. J. H. Sung, S. K. Lee, T. J. Yu, T. M. Jeong, and J. Lee, "0.1 Hz 1.0 PW Ti:sapphire laser," *Opt. Lett.* **35**(18), 3021–3023 (2010).
20. Y. Chu, X. Liang, L. Yu, Y. Xu, L. Xu, L. Ma, X. Lu, Y. Liu, Y. Leng, R. Li, and Z. Xu, "High-contrast 2.0 Petawatt Ti:sapphire laser system," *Opt. Express* **21**(24), 29231–29239 (2013).
21. M. E. Innocenzi, H. T. Yura, C. L. Fincher, and R. A. Fields, "Thermal modeling of continuous-wave end-pumped solid-state lasers," *Appl. Phys. Lett.* **56**(19), 1831–1833 (1990).
22. R. Weber, B. Neuenschwander, M. Mac Donald, M. B. Roos, and H. P. Weber, "Cooling Schemes for Longitudinally Diode Laser-Pumped Nd:YAG Rods," *IEEE J. Quantum Electron.* **34**(6), 1046–1053 (1998).
23. G. Wagner, V. Wulfmeyer, and A. Behrendt, "Detailed performance modeling of a pulsed high-power single-frequency Ti:sapphire laser," *Appl. Opt.* **50**(31), 5921–5937 (2011).
24. R. Berman, E. L. Foster, and J. M. Ziman, "The Thermal Conductivity of Dielectric Crystals: The Effect of Isotopes," *Proc. R. Soc. Lond. A Math. Phys. Sci.* **237**, 344–354 (1955).

## 1. Introduction

Ultra-high peak power laser systems are nowadays aiming to reach the few petawatt level output power [1]. With the use of even more advanced light sources of 10-100 PW peak power, electron beams can be accelerated to the TeV energy level, while the ion beams can reach the energy of up to a GeV [2]. This will allow to generate secondary sources of ultrabright X-rays and  $\gamma$ -rays [3]. These achievements could be widely applied to many areas of science, industry, medicine, homeland security etc. Wide applications, especially industrial ones, of ultrahigh peak power laser systems beyond basic scientific use are kept limited unless their repetition rate is reaching the (sub-)kHz regime. Since the energy of the pump pulse of a petawatt class laser exceeds few hundred joules, it results in a significant thermal load of the gain medium even at a low repetition rate.

The thin disk laser technology (TDT) that was intensively developed during the last decade for high average power and is applied mainly to CW and nano-picosecond systems, is able to alleviate thermal distortions and damages of laser crystals. It has also a potential to be used in systems with both high peak and average output power. With this technology the heat is extracted in the direction of beam propagation, across the whole aperture of the active medium. This allows a more effective and spatially uniform heat removal due to the significantly larger cooling surface compared to the conventional side-surface heat extraction. This method of cooling minimizes both thermal birefringence and lensing effects.

During the last two decades an incredible progress has been achieved in this technology. Using diode laser pumping the output power of up to hundreds of kW was demonstrated in a CW-regime, hundreds of millijoule energy with nanosecond pulses and a kHz repetition rate, and a joule energy level at 100 Hz with ps and sub-ps pulse durations (CPA systems) [4, 5]. Also the oscillators with tens of MHz repetition rate and sub-ps pulses were developed [6,7]. The amplification in thin-disk regenerative [8] and multipass amplifiers [9] can deliver pulses of a mJ- level with duration of several picoseconds and the average output power ranging from hundreds of Watts to a kW. Furthermore, this technology possesses the ability of further the output power and the energy to be scaled up by increasing the pump and the seed beam diameters. According to a theoretical prediction the TDT lasers can reach the output energy of several tens of joules with a larger disc diameter and the pump power [10].

The TDT has been exploited mostly for laser sources based on Yb:YAG or Nd:YAG active medium. The main advantage of these laser materials is the capability to be pumped by very effective diode pump lasers. Further, this combination supports small quantum defect that reduces consequently the dissipated thermal energy and the pump losses. Nevertheless,

the latter advantage also leads to a quasi-three level structure of energy levels, and thus to a large quenching of the signal wavelength and does not allow to increase the concentration of active ions. The high doping of active medium is also forbidden due to the associated dramatic growth of the transverse amplified spontaneous emission (TASE) and the transverse parasitic generation (TPG) [11, 12]. The low doping results in the low pump absorption and the low gain. This complicates the scheme of the amplifier and leads to multi-passing for both the pump and the seed.

Additionally, the active media used up to date with the TDT has narrow emission spectra. This limits the output pulse duration to the sub-ps range. Shortening the pulse duration and increasing the peak power requires active medium with a broad emission spectrum. Similarly, increasing the gain requires the medium with a high concentration of active ions and a large emission cross section. The most promising crystal with physical and spectroscopic characteristics that meets the above mentioned requirements is Ti:Sa. Moreover, it has several advantages, such as the high thermal conductivity (35W/mK for sapphire and 10 W/mK for YAG at room temperature). With doped crystals the difference of thermal conductivity will be even higher. It was shown, that doping with  $\text{Yb}^{3+}$  ions decreases the thermal conductivity of YAG at room temperature substantially (to 4.7 W/mK with 20% of Yb). At the same time, the concentration of Ti - ions in commonly used Ti:Sa crystals is only a fraction of a percent. This can't change the host - lattice thermal conductivity significantly [13]. The higher thermal conductivity of Ti:Sa could both compensate for a higher quantum defect, and also allow using thicker crystals. The thermal conductivity of sapphire is strongly temperature dependent. This property is successfully used in some of high peak power laser systems where the active medium is cryogenically cooled (Amplitude Technologies). As an example the thermal conductivity at 77 K is  $\sim 1000$  W/(mK) and it further increases to 6000 W/(mK) at around 40 K. This is more than two orders of magnitude higher than the conductivity at room temperature and is substantially higher than that of metals.

In this paper we present a theoretical study of a new technology (EDP-TD) that is a thin disk amplifier using a Ti:Sa medium combined with the method of extraction during pumping (EDP) [11] aimed to overcome the afore-mentioned limitations [14]. Contrary to the conventionally used technique when all the pump energy arrives prior the seed, the main idea of the EDP method is the temporal distribution of the pump in a multipass amplifier running close to saturation such that the TASE losses do not have time to increase substantially between the passes of the seed through the active medium. The major goal of the thin disk technology, as follows from its name, an efficient removal of heat requires reduction of the crystal thickness. High peak power, on another hand demands the large aperture of final amplifiers. This combination keeping the axial gain constant leads to an increase of inversion losses through TASE and TPG. Thus, the tradeoff between these effects creates an optimal configuration that must be found for the maximally efficient operation at both the high peak and the average powers.

## 2. The EDP-TD method of amplification

Ti:Sapphire ultra-high power lasers with tens of PW output power would have a kJ- energy level. The current technology of the Ti:Sa crystal growth supports the crystal diameter of 20 cm and the thickness in the range of several cm. Because of the substantial quantum defect, the Ti:Sa amplifiers are subjected to the thermal load of  $\sim 40\%$  of the pump energy. TASE and TPG are strongly dependent on the axial gain and the ratio of diameter of the pumped area to the crystal thickness [12]. For thin Ti:Sa active media these effects cause significant depletion of the inverted population, and hence limit the extracted energy and the repetition rate. It was demonstrated also in [11] that TASE restricts the energy storing and extraction in larger gain apertures even stronger than TPG. The threshold for the latter effect can be increased with the development of new index matching materials for cladding absorbers. Since Ti:Sa is a birefringent media, the full index matching cannot be reached simultaneously for both

ordinary and extraordinary polarized light. Despite that the value of the  $\sigma$  cross-section is 0.4x of the  $\pi$ , at high aspect ratios TASE and TPG can become a severe problem. Since the thickness of active elements is fixed to several centimeters, at a large aperture of the pump area the TASE typically limits the stored energy to 20-30%. As was shown in [15,16], this limit can be mitigated with the use of EDP which significantly reduces parasitic losses associated with both the TASE and the TPG, making EDP-based final laser amplifiers an excellent candidate for the new generation of CPA-laser systems [17]. The EDP-method was successfully applied in several Ti:Sa-based PW-class final amplifiers, where the output energy was in excess of 72 J and the currently record peak power of 2 PW in a single channel was demonstrated [18–20]. More recently, the authors of the paper [20] achieved the new impressive result of extracting 192 J by replacing the crystal in the last EDP-amplifier a bigger aperture one [1]. With the existing technology EDPCPA-systems are able to reach the kJ-level output energy and even several kJ when crystals of a larger aperture for duty amplifiers will be available [16].

As mentioned above, TDT is able to overcome another limitation of the high peak power laser systems on the repetition rate and hence can increase their average power. Making the active medium thin reduces the longitudinal gain, which can be compensated by increasing the doping. Nevertheless, the attempt to increase the longitudinal gain by raising the concentration of active ions and/or using crystals with higher emission cross section leads to a dramatic growth of the gain in the transverse direction of the active medium and consequently to big losses, and finally an inability to store the pump energy due to TASE [11].

The transversal gain in Ti:Sa has the highest value for the extraordinary light and is strongly dependent on the aspect ratio  $A = d/L$  of the crystal (where  $d$  - diameter of the pump area,  $L$  - crystal thickness), the longitudinal gain, and the angle relative the normal to the crystal surface (normally cut crystals that are used in power amplifiers are considered) [12]. This dependence for the crystal with absorption of the pump of 93% is shown in Fig. 1 for different values of the aspect ratio. One can see that the highest gain is achieved at the angle of total reflection that for Ti:Sa equals  $\sim 35^\circ$ . If the pump absorption exceeds 96.5% the major

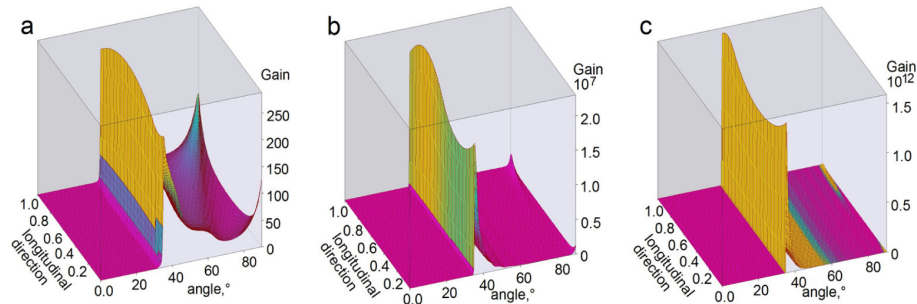


Fig. 1. Dependence of the transverse gain inside the Ti:Sa crystal on the angle between the longitudinal direction (normal to the crystal input surface) and direction of the ASE ray inside the crystal. The crystal is normally cut. The rays propagate in the plane that is perpendicular to the C-axis of the crystal and goes through the center of the pumped region. They start at the edge of the pumped region. Longitudinal gain  $G_l = 6$ , a – aspect ratio  $A = 2$ , b-  $A = 6$ , c –  $A = 10$ .

part of absorbed pump is concentrated close to the crystal surface, then the highest transverse gain corresponds to the case when the angle equals  $90^\circ$  (parallel to the crystal surface).

As follows from computer modeling shown in Fig. 1, the values of the transverse gain can reach extreme values (tens of thousands and higher). Under these conditions any reasonable index matching of absorbing media on side surfaces of the crystal for limiting the TPG threshold will not help to avoid big energy losses through TASE.

For the simplified case of a thin crystal when the pump absorption is low and the inversion is nearly uniform distributed in the longitudinal direction, one can derive a simple equation that describes dependence of the transverse gain  $G_t$  on the crystal aspect ratio,  $G_t = \exp(nA \ln G_l)$ , where  $G_l$  is the longitudinal gain,  $n$ -refraction index of sapphire. Here, as mentioned above, we take in to account that the maximum of the parasitic amplification is reached in direction perpendicular to the polarization of the amplified IR – beam and the angle of incidence equals the angle of total reflection. As seen from this formula a fivefold reduction of the crystal thickness keeping the longitudinal gain constant increases the transverse gain to the factor of 150.

The EDP-TD technique is suggested to be applied mostly in powerful final stages of ultra-high peak power laser systems with hundreds of Terawatts to tens of Petawatts power, which are operating in the saturation regime. In this case the crystal doping and the low signal gain do not play a significant role. On the one hand, since the extraction of energy is of major importance, the overall gain of the amplifier can be kept as small as  $\sim 10$ -20. On the other hand, the high energy level requires a large amplifier aperture. Contrary to ‘conventional’ TD amplifiers with the aperture of few millimeters when several tens of passes can be done easily [8,9], here power stages of the said Ti:Sa systems require a crystal size ranging from 5 to 20 cm. In this case the geometrical complexity and available space restrict the reasonable number of passes through the amplifier up to 6. These two requirements form the lower boundary for the saturated gain of 1.5-2, or the small signal gain of 3-5 per pass.

Figure 2 demonstrates dependence of the transverse gain on the crystal aspect ratio for different longitudinal small signal gain values, which correspond consequently to the absorbed pump fluence  $F$  of  $G_l = 10 - F = 3.8 \text{ J/cm}^2$ ,  $G_l = 7 - F = 3 \text{ J/cm}^2$ ,  $G_l = 5 - F = 2.5 \text{ J/cm}^2$  and  $G_l = 3.5 - F = 2 \text{ J/cm}^2$ . Two horizontal lines presented in the figure correspond to the maximum possible transverse gain suppression using a conventional method of the side surface cladding (solid line) and its combination with the EDP-method (dashed line). In both cases the side surface cladding with a commonly used liquid absorber is considered. As seen from this picture the conventional method of transverse gain compensation supports the aspect ratio between 2 and 4, while the EDP-amplifiers can afford 8-15. This implies the ability of the latter one to increase the output energy up to 16 times.

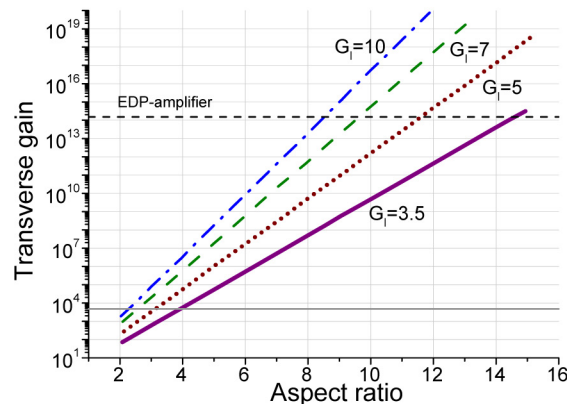


Fig. 2. Dependences of transverse gain on crystal aspect ratios.

From these calculations one can determine the maximum value of the aspect ratio and, depending on the required output energy, the crystal thickness. Then, depending on amount of pump passes the crystal doping that will support the required absorption and the small signal gain. For example, the highest aspect ratio which EDP is able to afford for the small signal gain of 3.5 is 15 with the reasonable amount of signal passes of 4-5. For a 10 PW laser (300J)

the Ti:Sa crystal of 15cm is required, this corresponds to the crystal thickness of 1 cm and doping according chosen pump absorption.

The EDP method can be applied to thin disks amplifiers in a similar way as it was done for conventional amplifiers [11, 15, 16]. In optimum conditions this method allows to significantly reduce (to 5-15%) the losses in the crystals with the big aspect ratio, or in thin disc crystals. Dynamics of losses during the crystal pumping with fluence of  $2 \text{ J/cm}^2$  per side for different aspect ratio values (1.5 - purple; 2.5 - red; 3.5 - green; 5 - blue) are presented in Fig. 3. This means that for the crystal with a 2 cm diameter and the thickness of 4 mm ( $A = 5$ ) the energy of the pump coming after  $\sim 35$  ns will be transferred not into the seed, but into the transverse lasing, thus the pump losses due to TASE will be more than 65%.

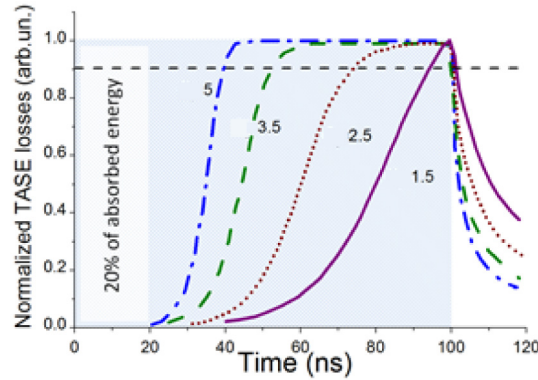


Fig. 3. Dependences of the losses during pumping for crystals with the different aspect ratios. Dashed area corresponds to the pump pulse.

As can be established from Fig. 3 the TASE losses require tens of nanoseconds to develop. In EDP-amplifier the inversion extracted by the seed passing through the active medium is restored between passes by an additional pumping up the crystal below the TASE anomalous losses point (straight dashed line in Fig. 3, which is the parasitic lasing threshold). The EDP method requires an extended pump-pulse duration ranging from tens to hundreds of nanoseconds, or a train consisting of several delayed shorter pulses. EDP can then be naturally combined with thin disc amplifiers. With Ti:Sa crystals of regular doping because of a smaller crystal thickness a smaller portion of the pump energy can be absorbed per pass. Multi-passing the pump the optimum EDP can be adjusted by choosing the correct distances of the pump and the seed pass shoulders.

In the following we demonstrate that the combination of EDP and TDT can open a new line of the CPA ultra-high intense high average power laser systems with a possibility to be scaled up to tens of a PW peak power and hundred Hz- repetition rate.

As an example, we have calculated losses in a 20x2 mm Ti:Sa crystal pumped with 11J (532nm, 100ns) and seeded by 180mJ using the method elaborated in [11]. We made some modification of the computer model connected with several simplified assumptions. If we choose a 2mm thick crystal with a high reflective coating for pump wavelength at one of the flat faces, only 3-5 passes (depending on the doping) will be enough to achieve effective absorption, wherein the distribution of pump irradiation in thickness of crystal will be very uniform (difference is within 3%). Taking into account the super-Gaussian pump energy distribution in the transverse direction we can assume the uniformity of population inversion density through the crystal volume.

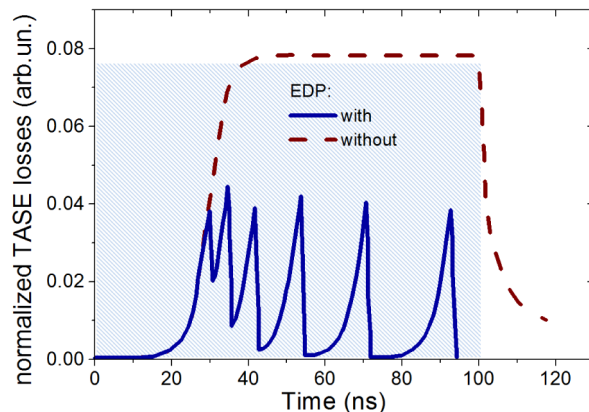


Fig. 4. Losses calculated for the 200 TW/100 Hz 6-pass Ti:Sapphire EDP- power amplifier. Shaded area is the pump pulse.

According to these calculations, the output energy for a EDP-amplifier is 6J for the input energy of 180mJ. TASE loss without EDP is  $\sim 80\%$  (dashed curve in Fig. 4), while energy loss with EDP is  $\sim 10 - 15\%$  (solid curve). With the extracted optical energy of about 6J, pulse duration of 15-30fs and compressor transmission efficiency of 70%, the peak power of the laser can reach 120-260TW, while the average power is close to 0.6 kW at the repetition rate of 100 Hz.

Now let us evaluate the ability of this amplifier to dissipate the heating energy. In general the nonlinear non-uniform 3D parabolic partial differential equation has to be solved for calculating the heat distribution in the crystal. This will be done in the next part of the paper. Here we make a rough estimation assuming the constant distribution of heat sources in the bulk of the crystal due to the very uniform distribution of the pump. Besides that, the temporal scale of pumping (within 100ns) is significantly shorter than the heat relaxation, so we can employ the uniform 1D heat-transport equation for our preliminary estimation, which is  $de/dt = -d\phi/dx$ , with constant initial and boundary conditions. Here  $e$  is the heat energy density,  $\phi$  is the heat fluence,  $t$  - the time variable,  $x$  - the space variable, and  $e = \rho c u$ ,  $\phi = k \cdot du/dx$ , where  $u$  is the temperature,  $c$  - the heat capacity,  $\rho$  - the density,  $k$  - the thermal conductivity, respectively. Suppose that the steady-state condition ( $de/dt = 0$ ) with the crystal temperature of  $60^\circ\text{C}$  (which is safe for such kind of laser crystals) has been reached. We consider that  $d\phi/dx = 0$  and  $\phi = \text{const}$  or equals the heat energy extracted between two shots. On the other hand since  $\phi = k \cdot du/dx$ , we can estimate time between shots required to extract this energy by this heat fluence. The temperature of coolant is taken  $\sim 5^\circ\text{C}$ , which could be provided by a conventional thermostat, and the energy transmitted into heat after each shot is 5 J. Suppose  $du = 55^\circ\text{C}$ ,  $dx = 1.5 \text{ mm}$  (center of the thickness) and  $k = 0.5\text{W/cm}\cdot\text{K}$  at  $5^\circ\text{C}$ ,  $\phi = 183\text{W/cm}^2$  and, taking into account the area of the crystal ( $7 \text{ cm}^2$ ), we get that the time of relaxation is 4 ms that corresponds to the repetition rate of 250Hz.

Further increasing these parameters is possible by reducing the coolant temperature. With cryogenically cooled Ti:Sa crystals at the temperature  $\sim 80\text{K}$  and the same crystal size, it will be possible to achieve the repetition rate approaching tens of kHz, or hundreds Hz with the largest existing today crystals (20cm diameter, 2 cm thickness).

In the following sections, the more detailed calculations of the 3D heating energy distribution within bulk of the crystal for different operation regimes are presented.

### 3. Description of thermal model

Thermal load in the amplifier crystal is in general calculated basing on the assumption that the heat is generated in case of all transitions between the electronic states of the Ti:Sa crystal, except the one that is associated with lasing (quantum efficiency for the given pump and the

seed wavelengths). However, for a more precise calculation, it is mandatory to know the efficiency of the specific amplifier. This way we can define a heat term that includes also the heat generated from the part of the stored energy which is not extracted by the seed, or by parasitic processes.

We have created a 2D axisymmetric model by using COMSOL Multiphysics software package (finite element method, FEM). Because of the 2D geometry, we could save computational power and time to optimize our designs. The temperature distribution  $T(r,z,t)$  inside the given material at arbitrary time points can be calculated by solving the time dependent heat equation, which is defined as

$$\rho C_p \frac{\partial T}{\partial t} = \nabla(k\nabla T) + Q_v, \quad (1)$$

where  $\rho$  is the density,  $C_p$  is the specific heat,  $k$  is the thermal conductivity of the material, and  $Q_v$  is the volumetric heat source term [21–23]. Temperature peaks caused by pump pulses can be calculated by using a time dependent analysis for the defined geometry. By resolving the heating in time, without losing the compactness of our model, only relatively low repetition rates (below 100 Hz) are accessible. For high repetition rates, the time required to obtain the steady state temperature distribution is growing and the minimal number of pulses that have to be modeled is beyond the practical limits. Thus, both the time dependent model and the stationary model are considered here as follows. Temporally resolved heating was calculated only in the case of low repetition rate systems to get information about the thermal dynamics of the amplifier heads. However, for our extensive, systematic investigation on the thermal limits of EDP-TD amplifiers, more compact calculations are required, which can be done by solving the stationary heat equation, that can be given in the form

$$\rho C_p u \cdot \nabla T = \nabla(k\nabla T) + Q_v, \quad (2)$$

where  $u$  is the velocity vector. Hereafter we define the heat source expression for both time dependent and stationary cases. For the time dependent model we defined a heat source that accounts for spatial and temporal profiles of pump pulses. Considering the typically provided spatial profile of pump pulses in PW class amplifiers, the spatial profile was assumed to be flat-top. Temporal profile of the pump pulses was defined to be Gaussian with full width at half maximum of 100ns. The heat source term for two side pumping and arbitrary spatial and temporal beam properties was defined basing on [18–20], which is

$$Q_{v,TD}(r, z, t) = \alpha \eta P_{peak} \cdot [e^{-\alpha z} + e^{-\alpha(L-z)}] \cdot f_{spatial}(r, z) \cdot f_{temporal}(t) \cdot \frac{1}{A(z)} \quad (3)$$

where  $\alpha$  is the absorption coefficient,  $L$  is the thickness of the Ti:Sa crystal,  $\eta$  is the heat dissipation factor,  $P_{peak}$  is the peak power of pump pulses,  $f_{spatial}(r, z)$  is the normalized spatial intensity distribution,  $f_{temporal}(t)$  is the normalized temporal intensity profile of the pulses and  $A$  is the cross section of the pump beam inside the material.

In the stationary model the temporal characteristics of the pump beam were not taken into account, which results in a more efficient analysis of the thermal limits of the EDPTD method. The heat source term in this case can be defined as

$$Q_{v,S}(r, z) = \alpha \eta P_{peak} \cdot [e^{-\alpha z} + e^{-\alpha(L-z)}] \cdot f_{spatial}(r, z) \cdot \frac{1}{A(z)} \quad (4)$$

where  $P_{peak}$  is the power of the pump beam, and the two side pumping is also assumed. Expressions (3) and (4) can be modified to describe multiple passes through the gain medium.

The temperature boundary condition was used at the boundaries, where materials are in contact with the heat sink, thus these boundaries are kept at constant temperature (coolant



temperature). This approximates an optimal condition of perfect cooling. In case of the mount-crystal contact boundaries, a highly conductive layer boundary condition was applied, assuming an indium foil standing between the two materials. At the boundary, where the Ti:Sa and the mount are in contact with air, a convective heat flux condition was used with  $10 \text{ W}/(\text{m}^2\text{K})$  heat convection coefficient, that is in good agreement with standard laboratory conditions. In case of cryogenic cooling, all boundaries except the cooled ones are taken to be thermally insulated (contact with vacuum). Meanwhile, the temperature dependence of thermal properties of Sapphire were taken into account basing on the data presented in [24] and built in material data in the COMSOL software.

#### 4. Results of thermal simulations

The general aim of our modelling was to estimate capabilities of the EDP-TD method to extend TW and PW-peak power scale Ti:Sapphire amplifiers for a higher average power. The temperature profile inside Ti:Sa crystals was calculated for different pumping and cooling conditions.

First, the temperature field distribution was modelled for the case of an amplifier with the diameter of 20 mm and thickness of 2 mm. The crystal is pumped from one side by pump pulses with energy of 11 J at 100 Hz repetition rate. The back surface of the gain medium has a highly reflective coating for 800 nm and 532. This surface is cooled down and its temperature is held at constant 278 °K.

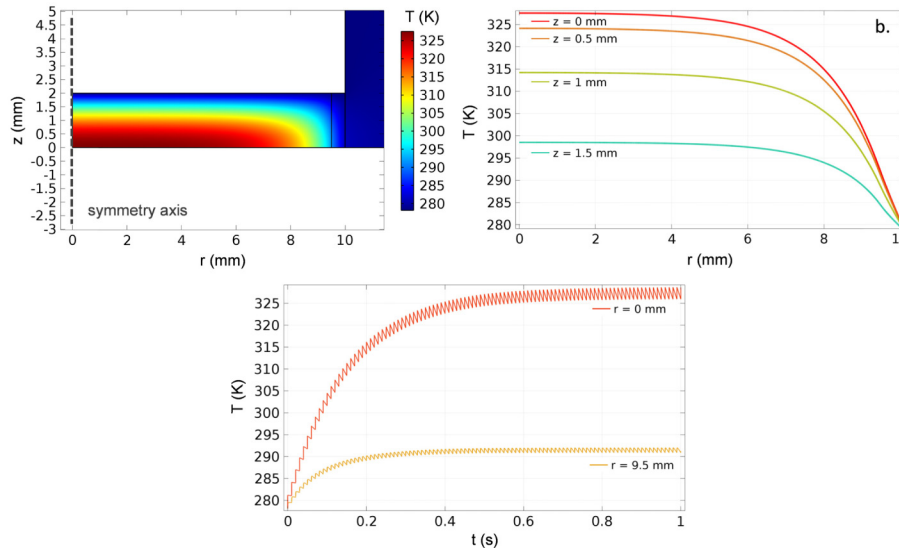


Fig. 5. Steady-state temperature distribution in a crystal with 2 mm thickness and 2 cm diameter (diameter of the pumped area is 1.9 cm) (a). Steady-state temperature profile in the transverse direction of the crystal for different longitudinal positions (from bottom to top) (b). Temporally resolved heating of 100 pulses producing the same steady-state temperature in the center (red) and at the edge of the pumped area (orange, below) of the crystal (c).

As a highly conductive layer we assumed indium in the form of a  $40 \mu\text{m}$  thick foil between the amplifier crystal and the copper mount. Total absorption of 95% of pump pulses energy could be reached with multiple passes through the crystal. As shown in Fig. 5(a) the peak temperature of  $327.6 \text{ }^\circ\text{K}$  was found in the centre of the crystal, while a relatively uniform profile along the transverse direction can be observed Fig. 5(b) displays the transverse temperature profile for different longitudinal position. Because of the finite diameter of the pump the temperature at the edge of the pump area dropped to  $278 \text{ }^\circ\text{K}$  quickly, however, the temperature profile was almost flat within the  $3/5$  of the radius.

Furthermore, the diameter of the quasi-flat area was bigger as the surface was closer to the coolant, this means thinner disk could be employed to achieve more uniform temperature distribution, but this also requires more passes for both the pump and the seed. Figure 5(c) shows that the central part of the crystal reaches the steady state within a longer time than the periphery part, and also with bigger temperature fluctuations of  $\sim 3\text{-}4^\circ\text{K}$ , which is acceptable for using the stationary model.

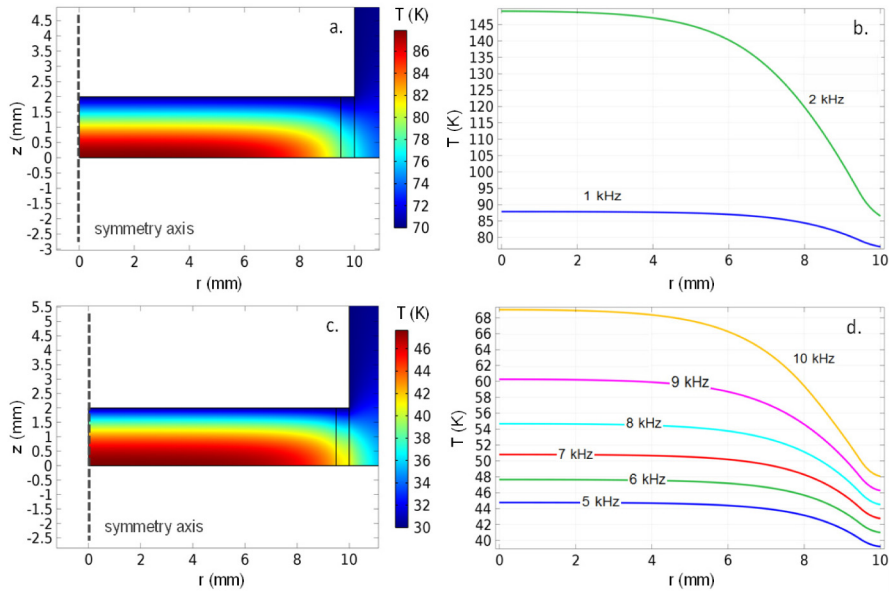


Fig. 6. Steady-state temperature distribution in case of the coolant temperature of 77 °K and 1 kHz repetition rate (average pump power is 1.1 kW) (a). Steady-state temperature profile along the front surface of the crystal in case of 1 and 2 kHz repetition rate and 77 °K coolant temperature (b). Steady-state temperature distribution in case of 30 °K coolant temperature and 6 kHz repetition rate (average pump power is 6.6 kW) (c). Steady-state temperature profile along the front surface of the crystal in case of repetition rates from 5 to 10 kHz and 30 °K coolant temperature (d).

High repetition rate amplification means much more pump power absorbed in the gain medium, consequently the use of a more effective heat extraction method is inevitable. Thus, we calculated the temperature field in the amplifier that was described in the previous paragraph, but with a cryogenic cooling and at a higher repetition rate (Fig. 6).

Calculations were performed for 77 °K (liquid nitrogen, Fig. 6(a) and 6(b), and also for 30 °K (liquid helium, Fig. 6(c) and 6(d)) coolant temperature to investigate the optimum conditions for cryogenic cooling. The maximum temperature difference in case of the 70 °K coolant temperature at 1 kHz repetition rate (1.1 kW pump power) is 18 °K, however in case of 30 °K coolant temperature, the same temperature difference is reached at 6 kHz repetition rate (6.6 kW pump power). It demonstrates that the repetition rate can be greatly promoted with a lower temperature coolant. Besides that the temperature dependence of refractive index of sapphire at lower temperature is getting much smaller. Hence, the wavefront of the amplified beam at cryogenic temperature after many passes can be kept nearly the same and no compensation of thermal lensing is necessary.

Large aperture Ti:Sa crystals with a high surface to volume ratio offer a good opportunity for efficient thermal management, and thus, can be considered as candidates to increase the repetition rate and hence the average power of laser amplifiers. Based on the proposed technology, a 2 PW peak power EDP-TD amplifier with a Ti:Sa crystal of 1 cm thicknesses and an aperture size of 11 cm was modelled. Water with temperature of 288 °K was taken as

the coolant material. Pumping was performed from the front surface with 120 J pulses at 10 Hz repetition rate, and a highly reflective coating for 800 and 532 nm was used on the back surface to reflect back both the seed and the pump pulses. Multiple passes (3-4 with a regular crystal doping) for the pump were applied to produce 95% of total absorption of the pump energy (Fig. 6(a) and 6(b)). The maximal temperature was found to be  $\sim 297$  K and the biggest temperature difference  $\sim 9$  K.

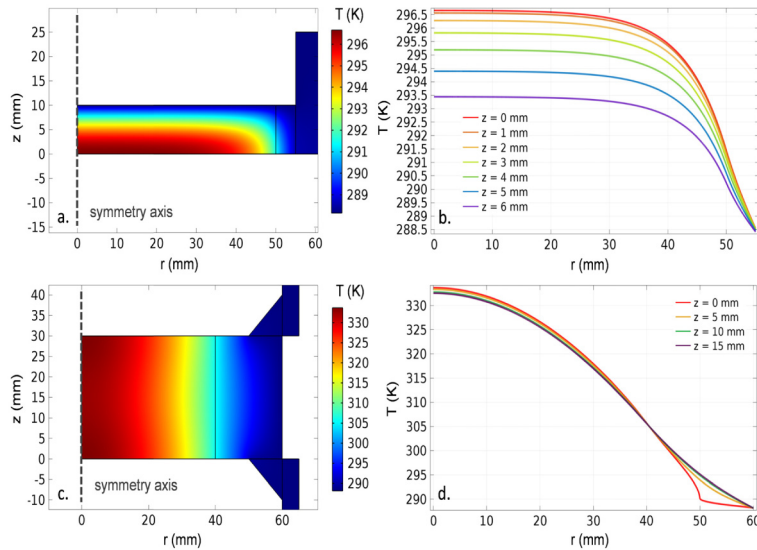


Fig. 7. a. Steady-state temperature distribution in the crystal with 1 cm thickness and 11 cm diameter for 120 J pumping at 10 Hz repetition rate (1.2 kW pump power) in case of 15 °C coolant temperature. b. Steady-state temperature profiles in the 1 cm thick crystal in the transverse direction for different longitudinal positions. c. Steady-state temperature distribution in the crystal with 3 cm thickness and 12 cm aperture size for 30 J per side pumping at 10 Hz repetition rate and side surface cooling with 15 °C coolant temperature. d. Temperature profiles in this crystal in the transverse direction for different longitudinal positions.

To compare with the EDP-TD amplifier the calculations were performed for a similar amplifier for a crystal of 3 cm thickness and 12 cm aperture. In this amplifier the crystal was cooled from the side surface, with water at 15 °C temperature. The amplifier media was pumped from both sides, each with 30 J [Fig. 7(c) and 7(d)]. As can be seen from the comparison of Fig. 7(b) and 7(d), a strong temperature gradient along the radial axis appears and the peak temperature is much higher in this crystal than in the EDP-TD case. This can cause a severe beam distortion after amplification. The simulation with pump pulses of 120 J shows a peak temperature of 385.5 K (112°C comparing to 23°C for the TD- amplifier) in the centre of the crystal with the coolant temperature of 15 °C.

We also modelled a 2 PW and a 10 PW peak power amplifiers for the case of cryogenic cooling with 77 K coolant temperature (liquid nitrogen), operated at 100 Hz and 10 Hz repetition rates, respectively.

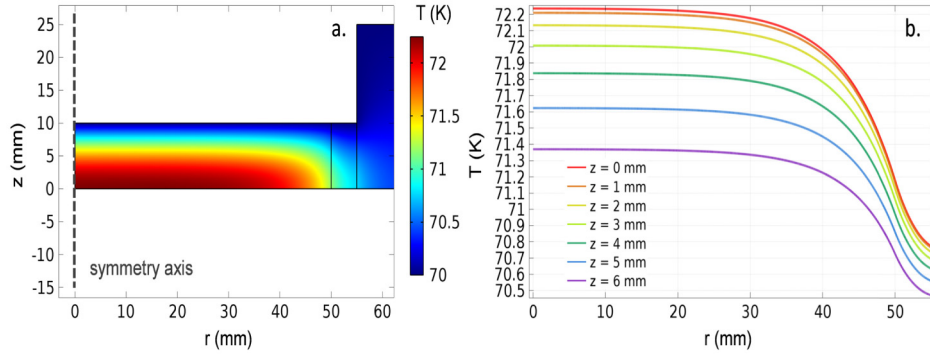


Fig. 8. a- Steady-state temperature distribution in the 2 PW, cryogenically cooled amplifier crystal with 1 cm thickness and 11 cm diameter for 120 J pumping at 100 Hz repetition rate (12 kW pump power) in case of 77 K coolant temperature. b. Steady-state temperature profiles for the 1 cm thick crystal in the transverse direction for different longitudinal positions.

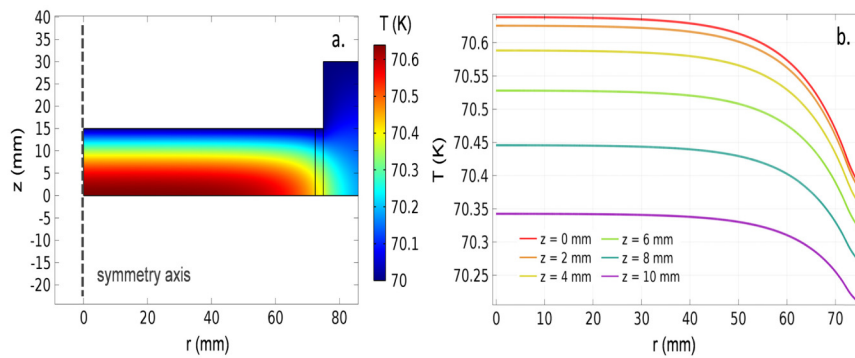


Fig. 9. a. Steady-state temperature distribution in the 10 PW, cryogenically cooled amplifier crystal with 1.5 cm thickness and 15 cm diameter for 500 J pumping at 10 Hz repetition rate (5 kW pump power) in case of 70 K coolant temperature. b. Steady-state temperature profiles in the 1.5 cm thick crystal in the transverse direction for different longitudinal positions.

Similarly to the crystals presented in Fig. 7(a) and 7(b), the pumping is performed from the front surface, and cooling is performed from the back surface of the gain medium, furthermore a highly reflective coating is assumed on the cooled surface of the crystal [Fig. 8. and Fig. 9]. The temperature distribution of these two cases is similar although the peak power has a factor of 5 difference. This shows a good scalability of this technology.

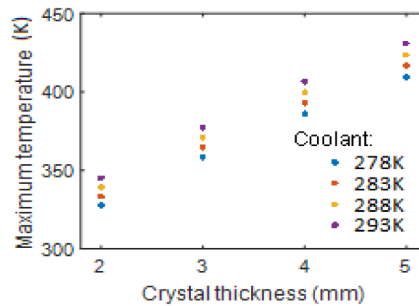


Fig. 10. Dependence of the peak temperature on thickness of the Ti:Sa crystal for different coolant temperatures.

Finally, Fig. 10 shows dependence of the disk temperature on the thickness calculated for different coolant temperatures. The amplifier diameter was 20 mm, thickness of the gain medium was varied between 2 and 5 mm, while the coolant temperature changed between 5°C and 20 °C. The crystal was pumped from one side by pump pulses with energy of 11 J at 100 Hz repetition rate. Rapid increase of the peak temperature is observed when the crystal thickness is increased by few millimeters only. This shows the importance of the aspect ratio (thickness) of the crystal.

We have analyzed the thermodynamic behavior of different crystal geometries in the broad range of the output power (from hundreds of Terawatts to tens Petawatts) and repetition rate (from tens of Hz to tens of kHz). As follows from the above examples, the increase of the peak temperature can be kept reasonable and the temperature distribution in the transverse direction can be done sufficiently uniform that ensures their low impact onto the quality of the amplified beam.

## 5. Conclusion

We have introduced a novel technology which allows high peak power Ti:Sa lasers of a PW class to be scaled towards high average power, even in excess of a kW level. This is the combination of the well-established thin disk technology applied to Ti:Sa amplifiers with the method of extraction during pumping (EDP-TD). This combination overcomes both the thermal effects in the final amplifier heads due to the high repetition rate of laser systems and the energy losses associated with TASE in thin crystals. The highest achievable possible aspect ratio of the amplifier crystal seems to be the major bottleneck of EDP-TD, limiting the highest possible extracted energy to the kJ level at few tens of Hz repetition rate. Nevertheless, the new method of laser architecture may open a new line of Ti:Sa CPA ultra-high intense, high average power laser systems with a possibility to be scaled up to tens of Petawatts peak power and tens of Hz- repetition rate.

## Acknowledgment

This research was partially supported by LASERLAB-EUROPE Project Acronym (ID) MBI002129, title “High Repetition rate Ti: Sapphire EDP-amplifiers.” (grant agreement no. 284464, EC-FP7).